

Analysis of a force reconstruction problem

E. Jacquelin[†], A. Bennani[‡] and M. Massenzio^{‡†}

Laboratoire Mécanique Matériaux Structures, Université Claude Bernard Lyon 1, 82 Bd Niels Bohr,
Domaine Scientifique de la Doua, 69622 Villeurbanne Cedex, France

(Received July 13, 2004, Accepted July 29, 2005)

Abstract. This article deals with the reconstruction of an impact force. This requires to take measurements from the impacted structures and then to deconvolve those signals from the impulse response function. More precisely, the purpose of the work described here is to analyse the method of deconvolution and the problems that it implies. Thus, it is highlighted that the associated deconvolution problem depends on the location of the measurement points: it is possible or not to reconstruct the force of impact in function of the location of this point. Then, the role of the antiresonances is linked up with this problem. The singular value decomposition is used to understand these difficulties. Numerical predictions are compared and validated with experiments.

Key words: inverse problem; impact force history; deconvolution; antiresonances.

1. Problematic

The determination of impact load history is necessary to design a structure. This step in the design process is often critical, but it is not always possible to instrument the impactor (impact of a bird on a windscreen, for example). Because it is necessary to recover the dynamic force using indirect measurements, the problem is then to deconvolve two signals.

These investigations have interested many researchers. Doyle (1984, 1987, 1989) wrote several papers in which he has described a frequencial method. Chang and Sun (1989), Yen and Wu (1995a, 1995b) and Liu (2002) for example, have preferred to work in the time domain. Gao and Randall (1999) use a cepstral analysis. A review of inverse analyse for indirect measurement of impact force has been proposed by Harrigan *et al.* (2001).

In fact, the authors recorded a strain response $S(M, t)$ at M ; then, to recover the load $F(I, t)$ induced by an impact at I , the authors must solve the following integral equation:

$$S(M, t) = G(I, M, t) \star F(I, t) \quad (1)$$

where $G(I, M, t)$ is the impulse response function between the points M and I ; \star is the convolution product: this is a deconvolution problem.

[†] Professor

[‡] Associate Professor, Corresponding author, E-mail: abdelkrim.bennani@iutb.univ-lyon1.fr

^{‡†} Associate Professor

To solve the Eq. (1), a discrete problem must be generated by sampling the convolution integral equation. This leads to a system of algebraic equations:

$$[\tilde{S}] = [\tilde{G}][\tilde{F}] \quad (2)$$

Where:

- $[\tilde{G}]$ is the transfer matrix:

$$[\tilde{G}] = \Delta t \begin{bmatrix} 0 & 0 & 0 & & 0 \\ \vdots & \vdots & \vdots & \vdots & \vdots \\ G(I, M, n_{shift}\Delta t) & 0 & & & 0 \\ G(I, M, (n_{shift} + 1)\Delta t) & G(I, M, n_{shift}\Delta t) & \ddots & & \\ G(I, M, (n_{shift} + 2)\Delta t) & G(I, M, (n_{shift} + 1)\Delta t) & \ddots & \ddots & \\ \vdots & \vdots & \ddots & \ddots & 0 \\ G(I, M, (n_{shift} + n - 1)\Delta t) & \vdots & \dots & \dots & 0 \end{bmatrix}$$

- $f_e = 1/\Delta t = 25600$ Hz is the sampling frequency,
- n_{shift} is such as $n_{shift}\Delta t$ is the elapse of the propagation time of the waves,
- $[S] = {}^t[S(M, 0), S(M, \Delta t), \dots, S(M, n_{shift}\Delta t), \dots, S(M, (n_{shift} + n - 1)\Delta t)]$ is the recorded strain with $S(M, 0) = S(M, \Delta t) = \dots = S(M, (n_{shift} - 1)\Delta t) = 0$: indeed at these times, the waves haven't reached yet the measurement point.
- $[\tilde{F}] = {}^t[F(I, 0), F(I, \Delta t), \dots, F(I, n_{shift}\Delta t), \dots, F(I, (n_{shift} + n - 1)\Delta t)]$ is the unknown load,
- t is the transpose operation.

In practice, the unrecorded response is not interesting. Therefore, the system of interest is:

$$[S] = [G][F] \quad (3)$$

Where:

$$\bullet [G] = \Delta t \begin{bmatrix} G(I, M, (n_{shift} + 1)\Delta t) & 0 & & 0 \\ G(I, M, (n_{shift} + 2)\Delta t) & G(I, M, (n_{shift} + 1)\Delta t) & \ddots & \\ G(I, M, (n_{shift} + 3)\Delta t) & G(I, M, (n_{shift} + 2)\Delta t) & \ddots & \\ \vdots & \vdots & \ddots & 0 \\ G(I, M, (n - (n_{shift} + 1) + 1)\Delta t) & \dots & \dots & G(I, M, (n_{shift} + 1)\Delta t) \end{bmatrix}$$

- $[S] = {}^t[S(M, (n_{shift} + 1)\Delta t), S(M, (n_{shift} + 2)\Delta t), \dots, S(M, (n - (n_{shift} + 1) + 1)\Delta t)]$
- $[F] = {}^t[F(I, 0), F(I, (\Delta t)), \dots, F(I, (n - 1)\Delta t)]$

Then, there is no row and no column of zeros in the matrix $[G]$.

To solve Eq. (1), one must deconvolve two functions. This is an inverse problem, which is well-

known to be ill-posed: generally, the solution is unstable (Alison 1979). This difficulty is often hidden in the literature on dynamic reconstruction of impact loads, even if its presence is implicit. Indeed, if sometimes the solving of Eq. (3) is realized with a conjugate gradient method (Chang and Sun 1989), (Yen and Wu 1995a), in some other cases, (Yen and Wu 1995b), (Tsai 1998) a gradient projection method is used to impose to the impact force to be nonnegative. In that latter case, one says the solution is obtained by regularization: the force is obliged to respect a supplementary condition to obtain a stable solution. Recently, an improvement of these regularization approaches has been proposed (Jacquelin 2003), (Liu and Shepard 2005). In this article, one will say that a force is recoverable if it is not necessary to regularize the problem to obtain an acceptable solution: a direct solving of Eq. (3) is sufficient.

No article on deconvolution in dynamics deals with the parameters which influence the ill-conditioning and then the reconstruction of the force. The purpose of this paper is to highlight the role of the location of the measurement point. To do that, some experiments are performed on a target which can be modelled analytically. First, the analytical model excited with numerical force is used: thus, the experimental noise is eliminated. In practice, the response S is numerically performed by applying Eq. (3) (forward problem) and, just after, without any signal processing, we try to solve the Eq. (3): this allow to evaluate if the force is recoverable or not. Finally, the real device will be tested to know if the first conclusions can be effectively applied.

In a previous article (Jacquelin *et al.* 2003) Thikhonov regularization was applied to time domain deconvolution for estimating the impact force acting on a plate. Note that the purpose of this article is to analyse a deconvolution problem with applications in dynamic and to highlight the critical parameters, the antiresonances. No method to recover the force will be suggested, even when the problem is rank-deficient.

2. The studied system

2.1 Experimental set-up

Experiments using an Al-5054 aluminium plate as a target were performed. The plate is circular (Fig. 1(a) - radius $a = 205$ mm; thickness $h = 5$ mm), clamped and isotropic (Young's modulus, Poisson's ratio and density are $E = 70$ GPa, $\nu = 0.3$ and $\rho = 2700$ kg/m³, respectively). The force is exerted at I , the center of the plate; the dynamic response is measured on the loaded surface by two strain gages positioned in the circumferential direction at 1 cm (M_1) and 5 cm (M_5) from the center of the plate (Fig. 1a).

We have chosen this device because an analytical expression for the transverse displacement can be obtained.

The schematic of the whole experimental setup is illustrated in Fig. 1(b). Data acquisition and analysis are made with a DSPT analyser (Siglab 20-42).

Experimental frequency response functions (FRF) are obtained by impulse testing performed with an impact hammer (B&K 8202). Moreover, a force-exponential window is used: a rectangular transient window function ("force" window) is applied to the input signal and an exponential window is applied to the output signal (McConnell 1995). In Fig. 2(a) and Fig. 2(b), the two FRF between I and M_i , $G_{i1}(\omega)$ and $G_{i5}(\omega)$ are plotted.

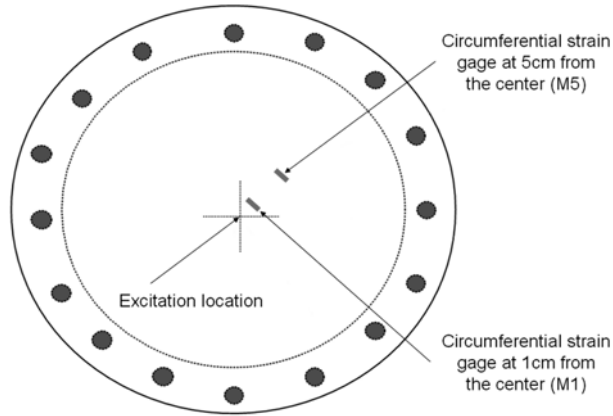


Fig. 1(a) Gages position

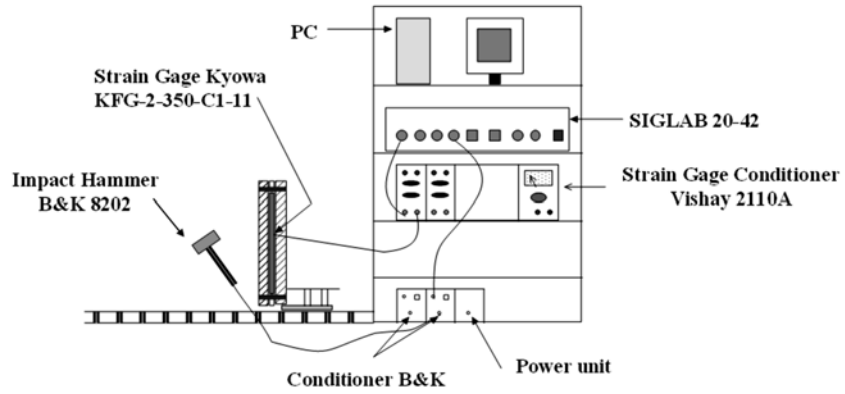


Fig. 1(b) Schematic of the experimental setup

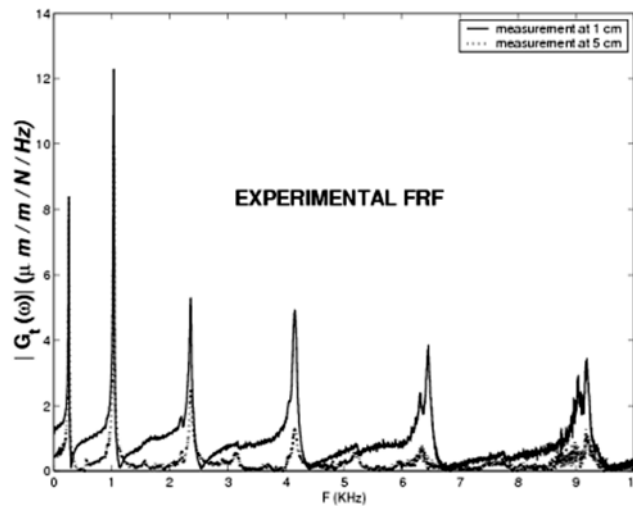


Fig. 2(a) Experimental frequency response function

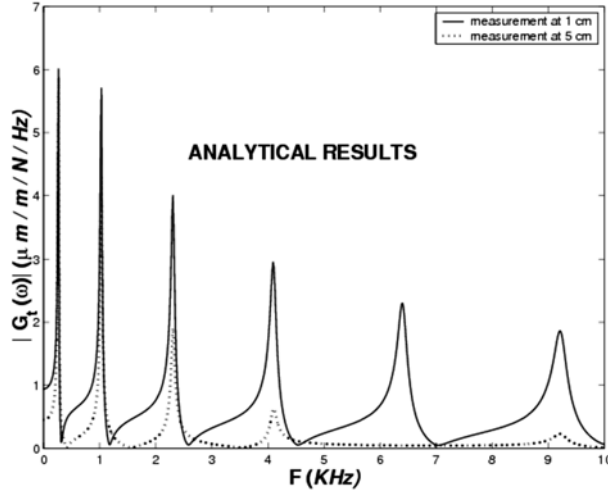


Fig. 2(b) Analytical frequency response function

Remark: $G_{t1}(\omega)$ and $G_{t5}(\omega)$ are in frequency domain: as the signals are in time domain, an inverse Fourier transform for those two FRF is involved. In this article, the same writing is used to designate a function and its Fourier transform: the variable t (resp. ω) indicates that one works in the time domain (resp. frequency domain).

2.2 Analytical modeling

The system is modeled by an elastic, circular embedded “Kirchhoff” plate with uniform characteristics, subjected to axisymmetrical load acting on its center. The equation of motion can be expressed in the following form (Graff 1975):

$$D\Delta\Delta w(r, t) + \rho h \ddot{w}(r, t) = q(r, t) \tag{4}$$

Where:

- $w(r, t)$ is the transverse displacement,
- $q(r, t) = f(t)\delta(r)$ is the applied loading at the center of the plate
- $D = \frac{Eh^3}{12(1 - \nu^2)}$
- $\Delta = \frac{1}{r} \frac{d}{dr} \left(r \frac{d}{dr} \right)$
- r, h, E, ν are respectively the radius and the thickness of the plate, the Young’s modulus and the Poisson’s ratio.

It is well-known (Graff 1975) that the mode shapes of such a plate under axisymmetrical loading are:

$$\phi_n(r) = J_0(\lambda_n r) - \frac{J_0(\lambda_n a)}{I_0(\lambda_n a)} I_0(\lambda_n r) \tag{5}$$

Where J_p and I_p are p -order first kind and first kind modified Bessel's function respectively; λ_n is a solution of the following characteristic equation:

$$J_0(\lambda_n a)I_1(\lambda_n a) + I_0(\lambda_n a)J_1(\lambda_n a) = 0 \quad (6)$$

By applying the modal superposition, the displacement $w(r, t)$ can be expressed in the following form:

$$\omega(r, t) = \sum_n \frac{1}{M_n \omega_{an}} \int_0^t \phi_n(0) \phi_n(r) f(\tau) \sin(\omega_n \sqrt{1 - \xi_n^2} (t - \tau)) \exp(-\xi_n \omega_n (t - \tau)) d\tau \quad (7)$$

M_n , ω_n , ω_{an} and ξ_n are modal mass, circular eigenfrequency, damped circular eigenfrequency ($\omega_{an} = \omega_n \sqrt{1 - \xi_n^2}$) and the damping ratio for the eigenmode n .

In this study, the strains in the circumferential direction ε_r on the surface of the plate ($z = h/2$) are recorded:

$$\varepsilon_r(r, h/2, t) = -\frac{h}{2r} \frac{d\omega}{dr}(t) \quad (8)$$

Then, the modal expansion of the impulse response function between the center of the plate ($r = 0$) and a measurement point located at r can be deduced:

$$G_r(r, 0, t) = -\frac{h}{2r} \sum_n \frac{\phi_n'(r) \phi_n(0) \sin(\omega_n \sqrt{1 - \xi_n^2} t) \exp(-\xi_n \omega_n t)}{M_n \omega_n \sqrt{1 - \xi_n^2}} \quad (9)$$

The analytical FRF plotted in Fig. 2(b) is then simply obtained by using the fast Fourier transform.

2.3 Remarks

1. The analytical modal expansion is interesting because it contributes to better understand the phenomenon.
2. All the considered modes are symmetrical.
3. Some adjustments of the numerical model are taken into account: the Young's modulus, experimentally determined from a tensile test, is adjusted to 70,6 GPa in order to match the experimental eigenfrequency.
4. The existence of damping in a structure affects the resonance and shifts the value of the FRF. In this model, the damping ratio used is the same for all the eigenmode. Its value is the one of the first eigenmode, identified from vibration tests. This assumption can explain some discrepancies among the experimental and numeric results.
5. The modal expansion must be truncated. An essential problem is that modal expansion slowly converges. Therefore, the number N of used eigenmodes must be sufficient to be able:
 - to represent the static flexibility $G_{r,static}$ of the plate correctly,
 - to well describe the dynamic behavior induced by the impact force.

Finally:

- the whole modes which are in the range of the excitation spectra must be retained,
- if the static flexibility is not well described, it is necessary to take into account the residual

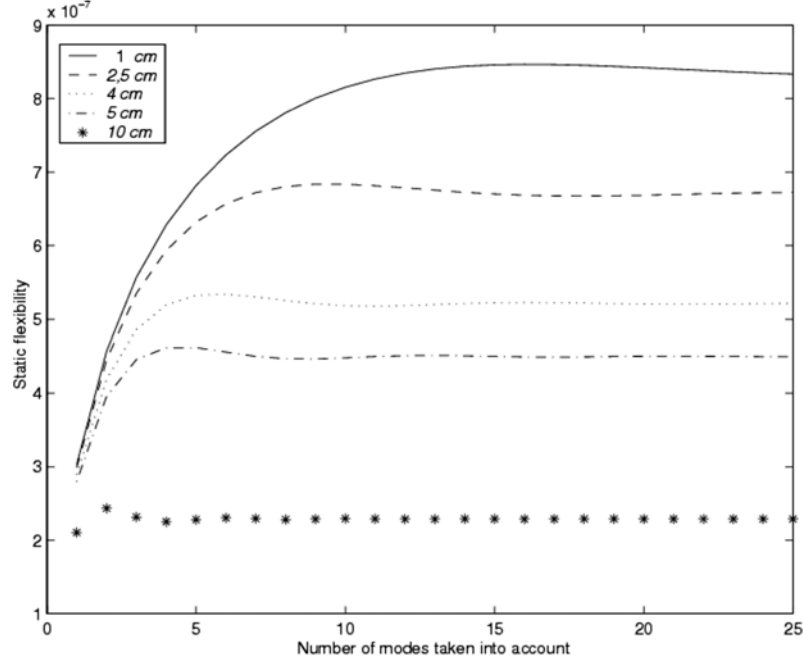


Fig. 3 Static flexibility

flexibility $G_{t \text{ residual}}$ (i.e., the flexibility of the neglected eigenmodes). Assuming that the neglected eigenmodes have a quasi-static response, the static and afterward the residual flexibility are determined from a static test, in order to take into account the participation of all the other modes:

$$G_{t \text{ residual}} = G_{t \text{ static}} - \frac{h}{2r} \sum_{n=1}^N \frac{\phi_n'(r)\phi_n(0)}{M_n \omega_n^2} \quad (10)$$

In these conditions, the deconvolution problem becomes:

$$S(r, t) = \int_0^t G_t^{\text{truncated}}(r, 0, t - \tau) F(\tau) d\tau + G_{t \text{ residual}} F(t) \quad (11)$$

Fig. 3, effectively shows that the analytical static flexibility is function of the number of modes retained in the expansion: few modes are sufficient if the measurement point is far from the center. In the following an impulse response function with $N = 7$ modes, corrected by the residual flexibility will be used.

2.4 Excitations

- **Numerical force:** the numerical impact force represented in Fig. 4 is built. It is then possible to obtain the response at any location of the plate by applying Eq. (1), i.e., a forward problem. The cutoff frequency of the force spectrum is less than the seventh eigenfrequency of the system. It is worth to note that the numerical force is well-known and not spoiled by any noise.

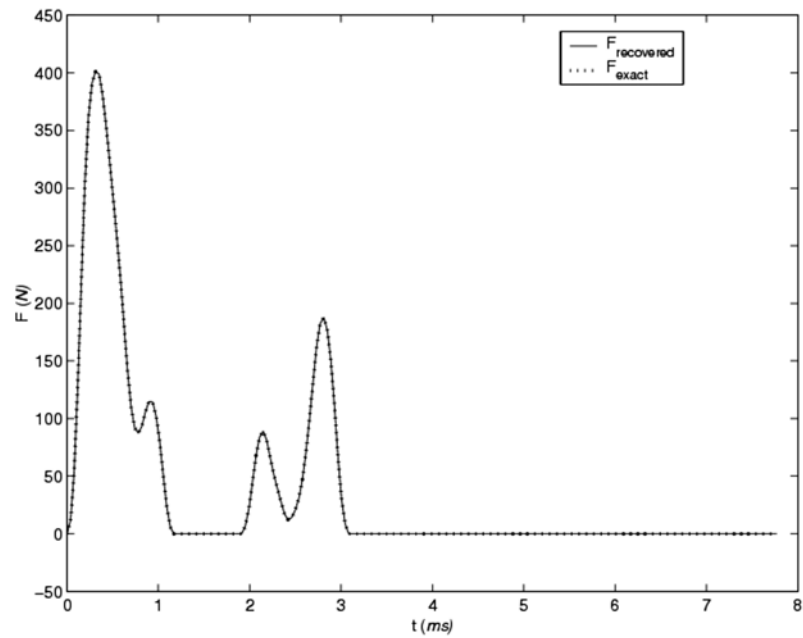


Fig. 4 Numerical initial and recovered forces – measurement point at 1 cm

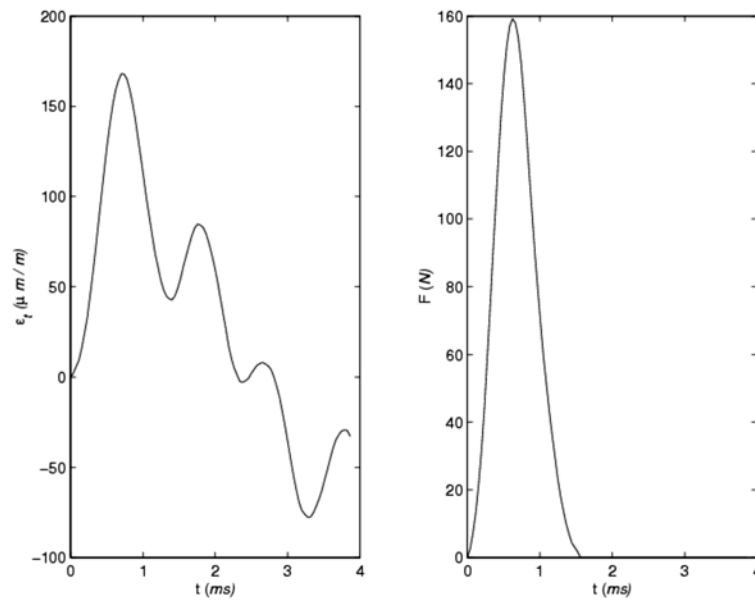


Fig. 5 Instrumented test: strain at 1 cm and force

- **Real force:** an instrumented hammer was used to impact the plate. The impact force acting on the plate and the strain induced by the sollicitation were simultaneously recorded (Fig. 5).

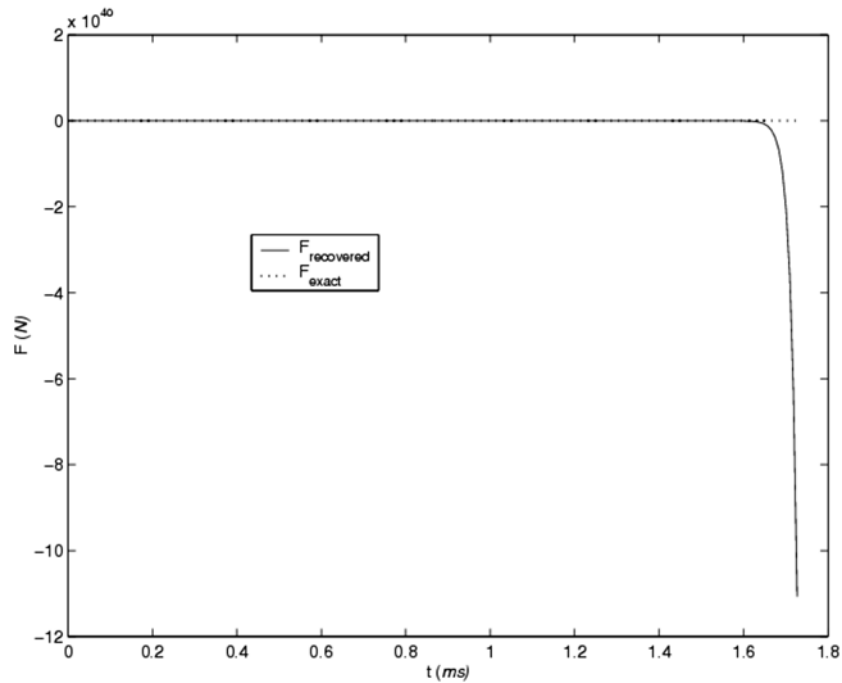


Fig. 6(a) Recovered force – measurement point at 5 cm

3. Analysis of the deconvolution problem

In this section, the model of the structure and the numerical force are used. A forward problem is carried out: both matrices $[G_{i1}]$ and $[G_{i5}]$ are multiplied by the numerical force $[F]$ and then the strains $[\varepsilon_{i1}]$ and $[\varepsilon_{i5}]$ are obtained. The problem is: is it possible to perform an inverse problem and then to recover the force?

3.1 Recoverable force?

To recover the force represented in Fig. 4, the linear algebraic system Eq. (3) is solved. The conclusion is dependent on the location of the measurement points.

Indeed, the solicitation can be perfectly recovered with the strains measured at 1 cm from the center, it is not the same with the point located at 5 cm, as seen in Figs. 4 and 6. Thus, it seems that the nature of the deconvolution problem is not the same in the two cases.

3.2 Nature of the deconvolution problem

A discretized deconvolution problem leads to ill-conditioned matrices. However, there is different kind of ill-conditioning (Hansen 1998): the problem can be ill-posed or can be rank-deficient.

To identify the nature of an ill-conditioning, it is interesting to use the singular value decomposition (SVD) of the $[G]$ matrix:

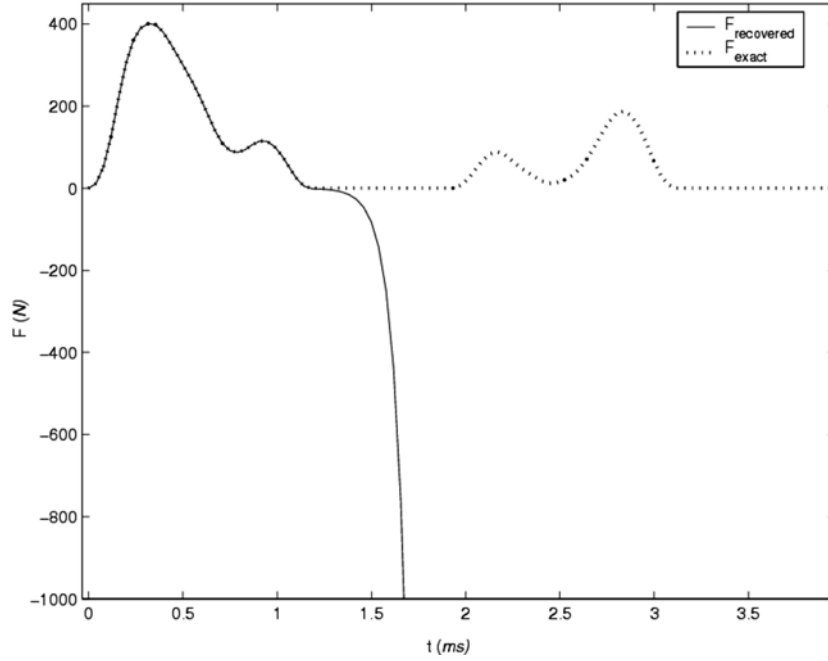


Fig. 6(b) Recovered force – measurement point at 5 cm

- the singular values decay gradually to zero with no particular gap: the problem is only ill-posed,
- the singular values decay gradually to zero and there is a well-determined gap between two singular values: the problem is rank-deficient.

In Fig. 7, the singular values of the matrices G_{t1} and G_{t5} are plotted. This figure highlights that the nature of the problem changes with the position of the measurement point:

- the inverse problem posed with G_{t1} is solely ill-posed,
- the inverse problem posed with G_{t5} is ill-posed and rank-deficient.

Therefore, we would conclude that G_{t1} contains more informations than G_{t5} .

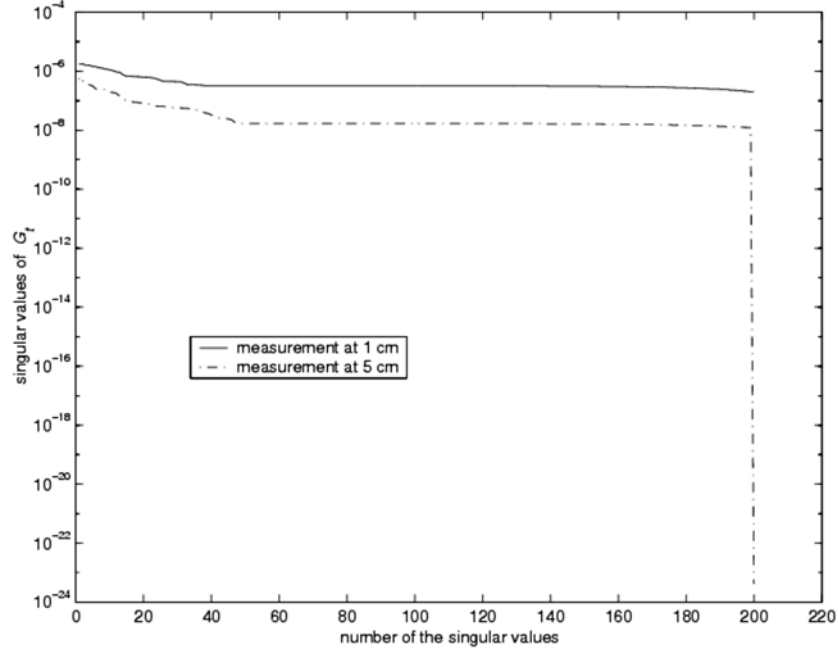
We recall that the SVD of a G , (m, n) , $m \geq n$ real matrix is defined as following:

$$G = U\Sigma^tV = \sum_{i=1}^n u_i \sigma_i^t v_i \quad (12)$$

Where:

- $U = (u_1, \dots, u_n):(m, n)$ is a matrix with orthonormal columns; u_i are the eigenvectors of U^tU ; u_i is a left singular vector of G ;
- $V = (v_1, \dots, v_n):(n, n)$ is a matrix with orthonormal columns; v_i are the eigenvectors of V^tV ; v_i is a right singular vector of G ;
- $\Sigma = \text{diag}(\sigma_1, \dots, \sigma_n)$ has nonnegative diagonal elements σ_i such as $\sigma_1 \geq \dots \geq \sigma_n \geq 0$; σ_i are the singular values of G : they are the square roots of the eigenvalues of the GG matrix.

Moreover, using the SVD, we can get a formulation of the solution of the problem Eq. (3) in the least square sense:


 Fig. 7 G_{t1} and G_{t5} singular values

If G is invertible, its inverse is given by $G^{-1} = \sum_{i=1}^n \frac{v_i^t u_i}{\sigma_i}$ and therefore the solution of the problem Eq. (3) is:

$$F = \sum_{i=1}^n \frac{u_i^t S}{\sigma_i} v_i \quad (13)$$

Otherwise, the pseudo-inverse G^* is given by $G^* = \sum_{i=1}^{\text{rank}(G)} \frac{v_i^t u_i}{\sigma_i}$ and the least square solution to the problem Eq. (3) is given by:

$$F = \sum_{i=1}^{\text{rank}(G)} \frac{u_i^t S}{\sigma_i} v_i \quad (14)$$

The expression Eq. (12) and the Fig. 7 explain why it is impossible to recover the force with the matrix G_{t5} : the smallest singular value is below the computer precision, therefore the results are dominated by rounding errors; that is not the case with G_{t1} .

3.3 FRF and force recovery

A such different nature between G_{t1} and G_{t5} is surprising: the points located at 1 cm and 5 cm from the center seem to be equivalent.

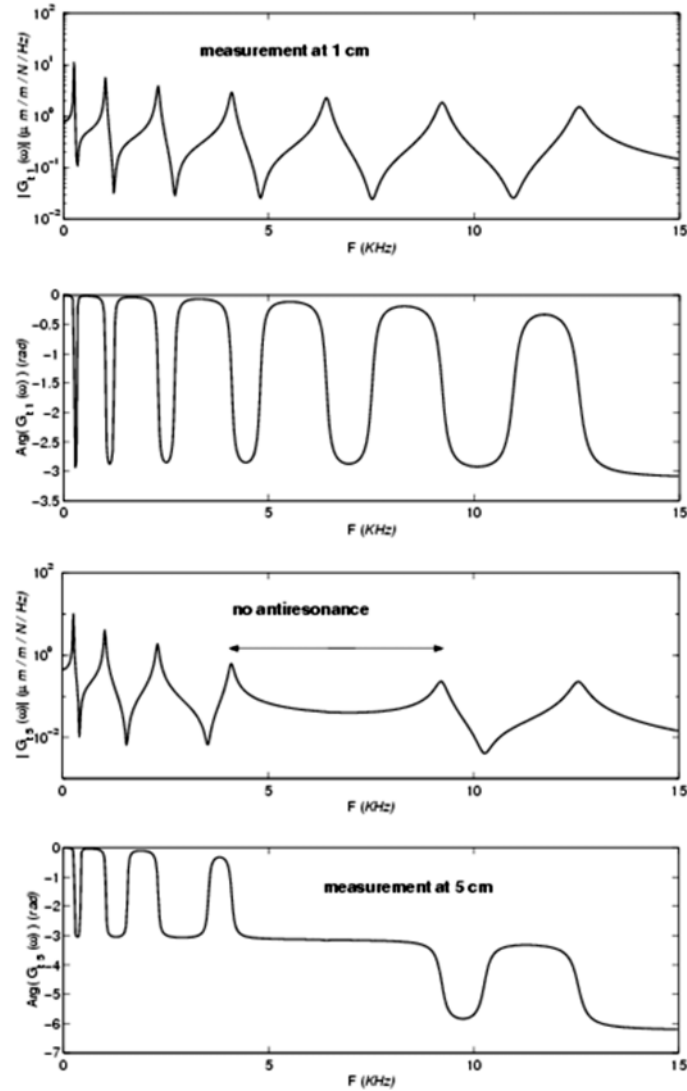


Fig. 8 Modulus and phase of G_{11} and G_{15}

However, a careful observation of the FRF modulus, $\|G_i(\omega)\|$, shows that (Fig. 8):

- G_{11} : there is always an antiresonance frequency between two successive resonance frequencies,
- G_{15} : there is not this succession of resonance and antiresonance frequencies.

Nota Bene: An antiresonance frequency ω_{ar} is well-defined for a system with no damping: the FRF modulus is null at this frequency, which is also a singular point of the curve; the FRF phase is broken. For a weak damping (it is the case in this study), the antiresonance frequency can be defined by a local minimum of the FRF modulus, which is a quasi-singular point (the slope of the curve has an important change at this frequency); the FRF phase is still broken.

For a forward problem, the resonances play a great role because they are the zeros of the FRF denominator. For an inverse problem, the antiresonance frequencies become the important parameters, as we can see, if we work in frequency domain. Indeed, Eq. (1) becomes:

$$S(\omega) = G_t(\omega) \times F(\omega) \tag{15}$$

then the solution is:

$$F(\omega) = \frac{S(\omega)}{G_t(\omega)} \tag{16}$$

For the inverse problem, the antiresonance frequencies play exactly the same role as the resonance frequencies for the forward problem.

But there is a great difference between a resonance and antiresonance: although the emergence of a resonance pick in FRF depends on the position of the sensor, the value of the resonances frequencies depend only on the structure, while the antiresonances are also a function of the position of the excitation and the measurement point. This can explain why the choice of the measurement point is so important to recover the force.

It is then natural to wonder if the existence of an antiresonance allows a better description of the structure. Indeed, when an antiresonance frequency is lacking between two resonances frequencies, the system becomes rank-deficient: it is exactly as if some information are redundant. Therefore, the forward and inverse problem are carried out with $G_{t5}^{4 \text{ modes}}$ an impulse response function between the center and the point located at 5 cm, but built with only 4 modes, and corrected by a residual

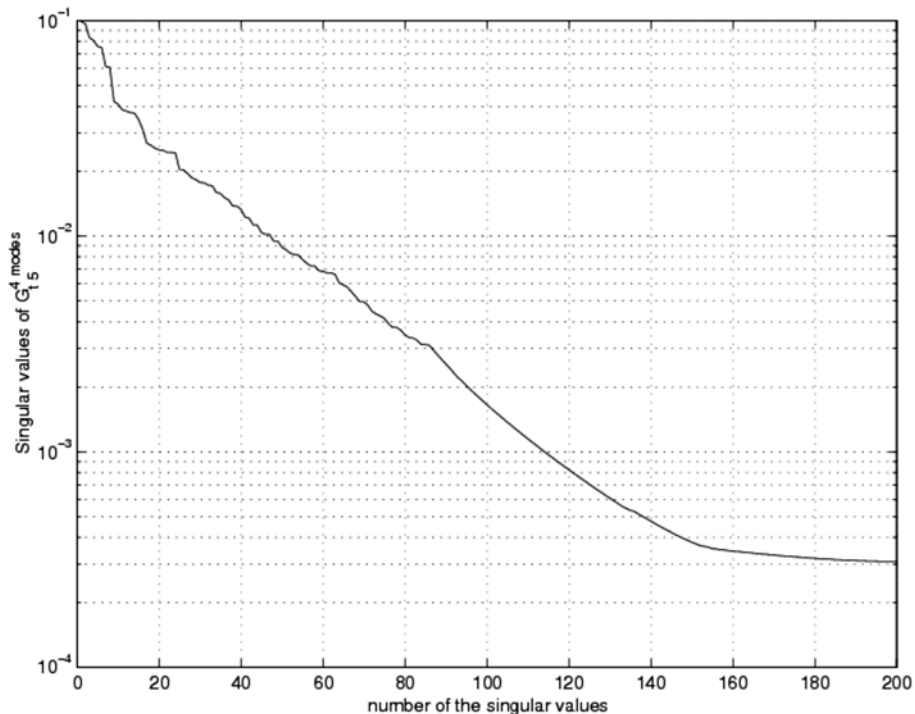


Fig. 9 Singular values of $G_{t5}^{4 \text{ modes}}$

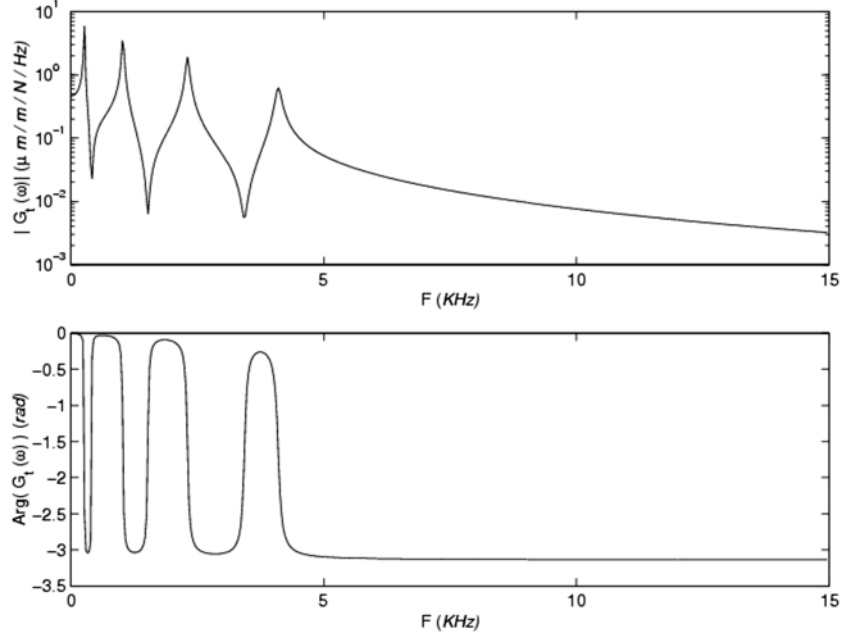


Fig. 10 Modulus and phase of $G_{15}^{4 \text{ mod es}}$

flexibility: in these conditions $G_{15}^{4 \text{ mod es}}$ gives less information on the dynamic of the system than G_{15} . But, in this case, the FRF as shown in Fig. 10, represent a succession of resonance and antiresonance frequencies; the SVD also proves that this matrix is not rank-deficient (Fig. 9). Then the force can effectively be recovered: the same result, previously plotted in Fig. 4, is found.

Therefore, the impossibility to recover a force with G_{15} is not a problem of information lack: this problem is certainly not a mechanical problem; only applied mathematicians could answer.

3.4 Number of time steps

Calculations were also performed with impulse response functions which simulate other sensors (Bennani 2001): for example $G_r(r, 0, t)$ is used to simulate radial strains:

$$G_r(r, 0, t) = -\frac{h}{2} \sum_n \frac{\phi_n''(r) \phi_n(0) \sin(\omega_n \sqrt{1 - \xi_n^2} t) \exp(-\xi_n \omega_n t)}{M_n \omega_n \sqrt{1 - \xi_n^2}} \quad (17)$$

The previous conclusions are not valid with G_{r5} (radial strain at 5 cm from the center of the plate): indeed, we can observe on Fig. 11 that there is not always an antiresonance between two resonances but it is possible to recover the force. In fact, in this case, when the number of time steps is 200, even if the smallest singular value is weak (3.10^{-7}), as shown in Table 1, it is not below the computer precision (10^{-16}): this is the reason why the force is recoverable.

But, as also shown in Table 1, if the size of the problem increases, i.e., if the total number of time steps increases (up to 800 for example), the lowest singular value (10^{-24}) is below the computer precision and the solution is dominated by rounding errors and becomes unstable: then, if a small

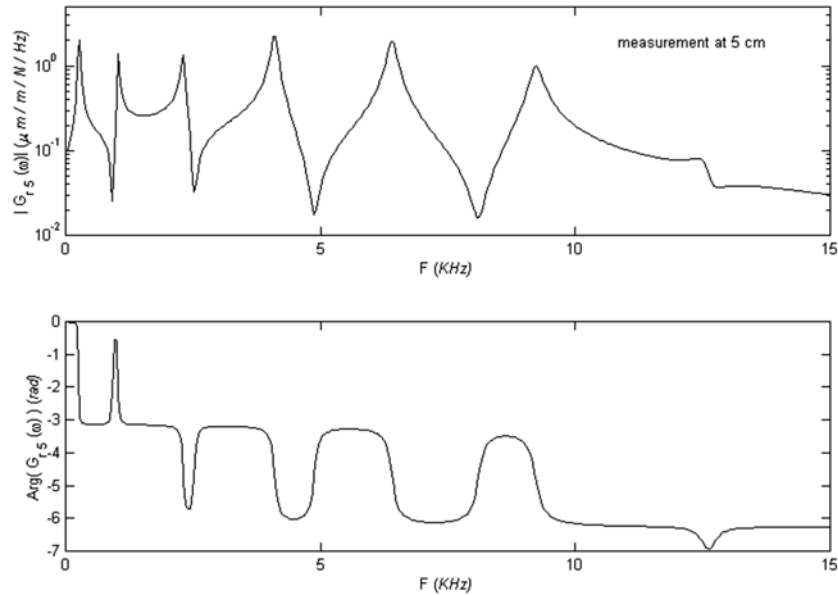


Fig. 11 Modulus and phase of G_{r5} - Number of time steps = 200

Table 1 Some singular values of different FRF

Number of time steps	G_{r5}		G_{r1}	
	Lowest singular value	Greatest singular value	Lowest singular value	Greatest singular value
200	$2.8 \cdot 10^{-7}$	$4.3 \cdot 10^{-6}$	$2.8 \cdot 10^{-7}$	$2.1 \cdot 10^{-6}$
800	10^{-24}	10^{-15}	$3.5 \cdot 10^{-8}$	$6.4 \cdot 10^{-6}$

sampling period is required for a forward problem to obtain some accurate results, this could induce an impossibility to recover the inverse solution.

It is worth to note that if the lowest singular value depends strongly on the number of time steps for the measurement at 5 cm, the size of $[G]$ has a very small influence on the condition number (i.e., the ratio of the greatest singular value on the lowest singular value) for the measurement point located at 1 cm, as shown in Table 1.

It has been shown that the role of the antiresonance does not depend on the nature of the sensor: accelerometer and displacement transducer have also been simulated and the conclusions are the same (Bennani 2001).

4. Experimental verification

The previous conclusions are made from some numerical signals and modeling. Then, it seems important to highlight also the role of the antiresonances with real signals. The experimental FRF G_{r1} and G_{r5} are determined (Fig. 2a) and then the instrumented impact test is realized as previously described.

To recover the impact force, the discrete convolution problem Eq. (3) is solved. Fig. 12(a) and Fig. 12(b) show that only the measurements at 1 cm allow the reconstruction, according to the numerical results. This validates the influence of the measurement point location.

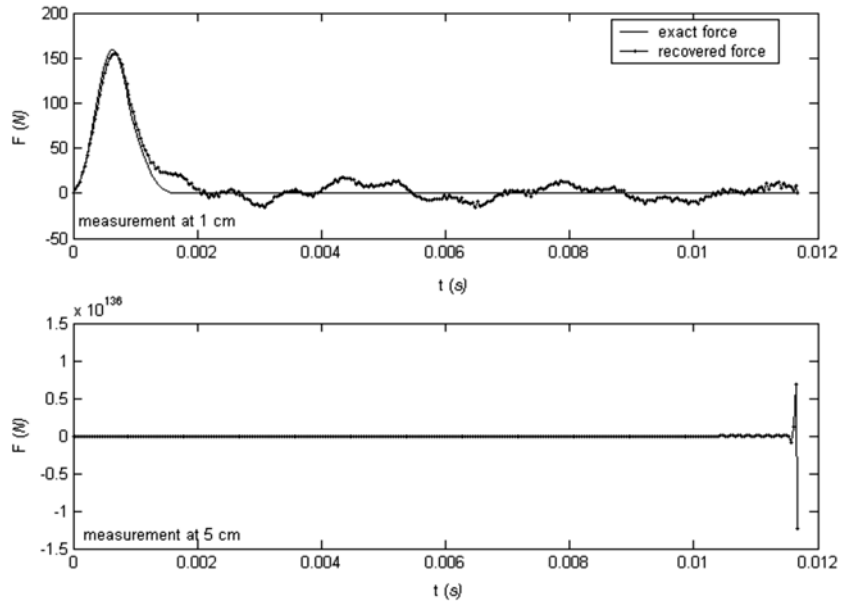


Fig. 12(a) Force reconstruction with experiment data

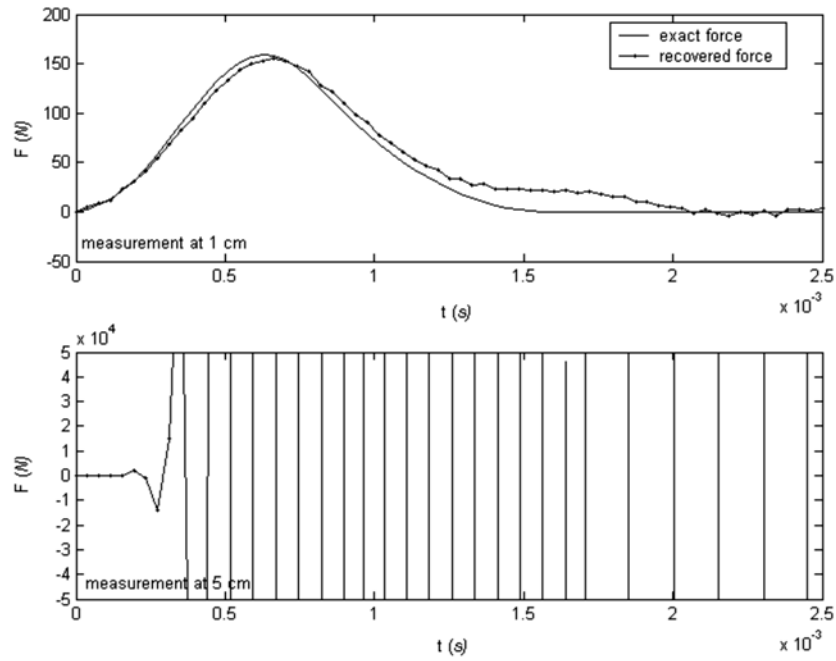


Fig. 12(b) Force reconstruction with experiment data - Zoom of the initial part

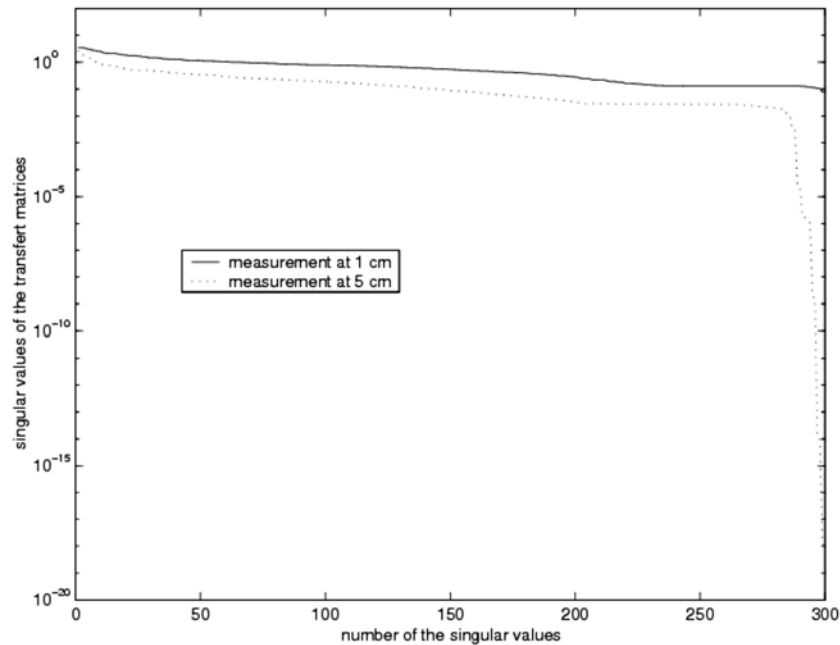


Fig. 13 Singular values of the experimental transfert matrices

Moreover, the SVD proves that the problem is rank-deficient and very ill-conditioned if we use the measurement point located at 5 cm (Fig. 13).

5. Conclusions

To recover an excitation by solving the algebraic system Eq. (2) is not so easy: the solution of such a system is not always stable. This study highlights the role of the antiresonances on the stability: a succession of resonance and antiresonance frequencies is required to be able to recover the force. Then, it seems important to choose well the location of the measurement point in order to obtain a good condition number of the transfer matrix. The reason why the lack of the antiresonance frequency causes the rank deficiency of the transfer matrix, is the subject of current researches.

We have also shown that the inverse problems are dominated by the rounding errors when the system is rank-deficient: then the number of calculus must not be high in order to succeed in recovering the force.

References

- Alison, H. (1979), "Inverse unstable problems and some of their applications", *Math. Scientist*, **4**, 9-30.
 Bennani, A. (2001), "Détermination par une analyse dynamique et une méthode inverse, de la fonction de chargement d'une structure", PhD Thesis, Université Claude Bernard-Lyon I-France.
 Chang, C. and Sun, C.T. (1989), "Determining transverse impact force on a composite laminate by signal

- deconvolution”, *Experimental Mechanics*, **29**(4), 414-419.
- Doyle, J.F. (1984), “Further developments in determining the dynamic contact law”, *Experimental Mechanics*, **24**(4), 265-270.
- Doyle, J.F. (1987), “Further developments in determining the dynamic contact law”, *J. Sound Vib.*, **118**(3), 441-448.
- Doyle, J.F. (1989), *Wave Propagation in Structures*, Springer-Verlag.
- Graff, K.F. (1975), *Wave Motion in Elastic Solids*, Dover Publications.
- Gao, Y. and Randall, R.B. (1999), “Reconstruction of diesel engine cylinder pressure using a time domain smoothing technique”, *Mechanical Systems and Signal Processing*, **13**(5), 709-722.
- Hansen, P.C. (1998), *Rank-deficient and Discrete Ill-posed Problems*, SIAM.
- Harrigan, J.J., Reid, S.R. and Inoue, H. (2001), “Review of inverse analysis for indirect measurement of impact force”, *Appl. Mech. Rev.*, **54**(6), 503-524.
- Jacquelin, E., Bennani, A. and Hamelin, P. (2003), “Force reconstruction: Analysis and regularization of a deconvolution problem”, *J. Sound Vib.*, **265**, 81-107.
- Liu, Y. and Shepard, W.S. (2005), “Dynamic force identification based on enhanced least squares and total least-squares schemes in the frequency domain”, *J. Sound Vib.*, **282**, 37-60.
- Liu, G.R., Ma, W.B. and Han, X. (2002), “An inverse procedure for identification of loads on composite laminates”, *Composites Part B*, **33**(6), 425-432.
- McConnell, K.G. (1995), *Vibration Testing - Theory and Practice*, Wiley Interscience.
- Tsai, C.Z., Wu, E. and Luo, B.H. (1998), “Forward and inverse analysis for impact on sandwich panels”, *AIAA*, **36**, 2130-2136.
- Yen, C.S. and Wu, E. (1995a), “On the inverse problem of rectangular plates subjected to elastic impact, Part I: Method development and numerical verification”, *J. Appl. Mech.*, **62**(3), 692-698.
- Yen, C.S. and Wu, E. (1995b), “On the inverse problem of rectangular plates subjected to elastic impact, Part II: Experimental verification and further applications”, *J. Appl. Mech.*, **62**(3), 699-705.